Multiple endpoints to evaluate pristine and remediated titanium dioxide nanoparticles genotoxicity in lung epithelial A549 cells

Andrea Stoccoro, Sebastiano Di Bucchianico, Fabio Coppedè, Jessica Ponti, Chiara Uboldi, Magda Blosi, Camilla Delpivo, Simona Ortelli, Anna Luisa Costa, Lucia Migliore

Multiple endpoints to evaluate pristine and remediated titanium dioxide nanoparticles genotoxicity in lung epithelial A549 cells

Andrea Stoccoro[a,b], Sebastiano Di Bucchianico[a], Fabio Coppedè[a], Jessica Ponti[c], Chiara Uboldi[a*], Magda Blosi[d], Camilla Delpivo[d], Simona Ortelli[d], Anna Luisa Costa[d], Lucia Migliore[a]

[a]*Department of Translational Research and New Technologies in Medicine and Surgery, Laboratory of Medical Genetics, University of Pisa, Via Roma 55, Pisa 56126, Italy,*

[b]*Doctoral School in Genetics, Oncology and Clinical Medicine, Department of Medical Biotechnologies, University of Siena, Siena, Italy*

[c]*European Commission, Directorate General Joint Research Centre, Directorate F – Health, Consumers and Reference Materials, Consumer Products Safety Unit (F.2), via E. Fermi 2749, 21027 Ispra (VA),*

[d]*Institute of Science and Technology for Ceramics (CNR-ISTEC), National Research Council of Italy, Via Granarolo 64, 48018 Faenza, (RA), Italy.*

**Present address: Biogenotoxicology, Human Health and Environment Unit, Mediterranean Institute of marine and terrestrial Biodiversity and Ecology (IMBE), Aix-Marseille University, Marseille, France.*

Correspondence:

Lucia Migliore, Department of Translational Research and New Technologies in Medicine and Surgery, Laboratory of Medical Genetics, University of Pisa, Via Roma 55, Pisa 56126, Italy

E-mail: lucia.migliore@med.unipi.it

Tel:+39 050 2218549; Fax: +39 050 2210624

Highlights

- *In vitro* effects induced by coated with silica or citrate TiO_2 NP were studied.
- Cytotoxicity, genotoxicity and epigenetoxicity of TiO_2 NP were investigated in A549 cells.
- TiO_2 NP resulted both cytotoxic and genotoxic, and coating strategy did not reduce adverse effects.
- Reduction of global DNA methylation levels was induced by all NP after 72h of treatment.
- Citrate coated TiO_2 NP induced the highest cytotoxic, genotoxic and epigenotoxic effects.

Abstract

Titanium dioxide nanoparticles (TiO_2 NP) are broadly used in a wide range of applications. Several studies have reported that TiO_2 NP possess cytotoxic and genotoxic properties that could induce adverse health effects in humans. The FP7 Sanowork project was aimed to minimize occupational hazard and exposure to engineered nanomaterials (ENM), including TiO_2 NP, through the surface modification in order to avoid possible adverse toxic effects for humans. In this study we investigated cytotoxicity, genotoxicity and epigenetic properties of TiO_2 NP uncoated and coated with silica or citrate, as well as of the benchmark material P25. We used a panel of *in vitro* assays in the human lung epithelial cell line A549, in order to better understand if the remediation strategy adopted was able to counteract possible toxic effects of uncoated TiO_2 NP. Our results showed that the uncoated TiO_2 NP were both cytotoxic and genotoxic, and the remediation strategy adopted did not reduce the adverse effects of uncoated TiO_2 NP. In particular, the presence of citrate was able to increase their cytotoxicity and genotoxicity, exerting also epigenotoxic effects, as evaluated by the marked reduction of LINE-1 methylation levels.

Keywords: TiO_2 nanoparticles; genotoxicity; epigenotoxicity

1. Introduction

Titanium dioxide (TiO_2) nanoparticles (NP) are manufactured worldwide in large quantities for the use in a wide range of applications such as photocatalysis, pigments and cosmetic additives (Aitken et al., 2010). TiO_2 NP possess different physicochemical properties compared to their fine particle analogs, which might alter their bioactivity. Numerous *in vivo* and *in vitro* studies have investigated the TiO_2 NP toxicity and the results are often controversial (reviewed in Chen et al., 2014). More recently it was observed that 6 months of inhalation of TiO_2 NP did not induce pulmonary inflammation in rats (Morimoto et al., 2016), and no signs of genotoxicity were detected in peripheral blood and liver of mice exposed to TiO_2 NP by intravenous injections for 4 consecutive weeks (Suzuki et al., 2016). The International Agency of Research on Cancer (IARC) classified TiO_2 as possibly carcinogenic to humans (Group 2B) based on sufficient evidence in experimental animals and inadequate evidence from epidemiological studies (IARC, 2010). Investigations in animal models support a carcinogenicity potential also for TiO_2 NP after intratracheal and inhalation exposure (reviewed in Shi et al., 2013). However, the exact mechanism of TiO_2 NP induced carcinogenicity is not clear. Several evidences indicate that TiO_2 NP are able to induce both cytotoxicity and genotoxicity in *in vivo* and *in vitro* model systems likely through the generation of reactive oxygen species (ROS), induction of inflammation and alterations in cell signaling transduction (Chen et al., 2014; Shi et al., 2013). Moreover, recent evidences clearly point to the ability of NP to induce epigenetic changes (Shyamasundar et al., 2015; Stoccoro et al., 2013). These toxic properties could play an important role in the etiology of TiO_2 NP carcinogenesis potential.

A pivotal role in the nanotoxicity field is to set up design rules for the synthesis of safe NP. The FP7 Sanowork project aimed to minimize occupational hazard and exposure to engineered nanomaterials (ENMs) through the surface modification of NP to prevent possible health effects. In the present study the proposed risk remediation strategies (RRS) consist of the surface coating of NP, with the aiming at decreasing both the toxicity and the emission of materials. The following NP

were investigated: pristine TiO_2, citrate coated TiO_2 and silica coated TiO_2 as well as the benchmark material Aeroxide P25. The target TiO_2 NP sample studied was involved in the processing line consisting in the application of TiO_2 nanosols to ceramic substrates through spray-coating, one of the most flexible methods for the application of nanostructured suspensions, allowing rapid and simple production changes. The critical step for health hazard and exposure assessment was actually the spray coating operation which could cause nanoaereosolisation and induce inhalation of NP. SiO_2 and citrate coatings were proposed for their potential to improve powder dispersability and hydrophylicity, positively impacting on mechanisms driving cellular toxicity (Nel et al., 2009).

In the present study multiple endpoints of cytotoxicity and of genotoxicity induced by pristine and remediated TiO_2 NP were investigated, focusing on their potential to induce impairment of cell capacity to form colonies and cell death, as well as different types of DNA damage. We also investigated the capacity of TiO_2 NP to induce a global DNA methylation effect by means of LINE-1 methylation analysis that is frequently used as a surrogate of global DNA methylation levels (Yang et al., 2004) and has been associated with genome instability (Cho et al., 2015; Luzhna et al., 2013). Since the respiratory tract is likely to be the main exposure route of TiO_2 NP, we investigated the toxicity of NP in A549 cells, a human alveolar type II-like epithelial cell line, that is an inhalation model system frequently used in nanotoxicity studies (Love et al., 2012).

2. Materials and methods

2.1. Preparation and characterization of TiO_2 NP

Commercial TiO_2 NP (84% anatase, 16% brookite crystal phase composition, Ortelli et al., 2013) were provided by Colorobbia Italia SpA as colloidal nanosuspension (nanosol).

The remediation process consisted in silica and sodium citrate coating. The following panel of NP were thus studied: pristine TiO_2, citrate coated TiO_2 and silica coated TiO_2. Furthermore, TiO_2 Aeroxide® P25 was used as benchmark material.

2.2. TiO_2 nanosols preparation

The silica modified TiO_2 NP was produced following the hetero-coagulation route: opposite charged TiO_2 NP and SiO_2 NP were diluted and then mixed together at room temperature, maintaining a SiO_2/TiO_2 weight ratio equal to 3 and a total solid content of 3 % wt. The obtained mixtures were ball milled for 24 h using 5 mm diameter zirconia spheres as milling media to obtain slightly cloudy solutions.

The citrate modified TiO_2 NP was produced by self-assembly strategy: trisodium citrate dihydrate was added to TiO_2 NP suspension (3 % wt) at room temperature and by employing a citrate/TiO_2 NP weight ratio equal to 0.83. The reaction mixture was stirred overnight resulting in a transparent and stable suspension.

2.3. Sol state characterization of TiO_2 NP

The physicochemical characterization of the pristine and modified TiO_2 samples was performed by using time, temperature, concentration and medium that closely simulated the experimental conditions used for cellular tests. The morphological analysis on pristine and modified samples was

performed by FEI titan TEM operating at an acceleration voltage of 300kV. One drop of diluted nanoparticle suspension in deionized water (30 μg/ml) was deposited on a film-coated copper grid and characterized. The colloidal characterization (hydrodynamic diameter and Zeta potential) were investigated for samples dispersed both in deionized water or complete cell culture medium (125 μg/ml) using light scattering optical technique (Zetasizer nano ZSP model ZEN5600; Malvern Instruments, UK). Further experimental details are provided in a recent paper (Stoccoro et al., 2016).

2.4. Cell culture conditions

Human alveolar epithelial type-II-like A549 cells were purchased, mycoplasma free, from the Istituto Zooprofilattico Sperimentale of Brescia (IZSBS; Brescia, Italy), and cultured in Ham's F12 medium (Lonza; Italy) supplemented with 10 % (v/v) fetal bovine serum EU standard (LonzaBioWhittaker® Sera; Italy) and 1 % (v/v) Penicillin (10,000 U/ml) Streptomycin (10,000 μg/ml) (Gibco Life Technologies; Italy). Cells were grown under normal cell culture conditions (37 °C; 5% CO_2; 95% humidity) and passaged weekly in tissue culture-treated flasks (Sarstedt; Italy). Uncoated, silica and citrate coated TiO_2 NP were provided as aqueous stock solutions at the nominal concentration of 30 μg/μl. The Aeroxide® P25 benchmark material was provided in powder form and resuspended in deionized water at the nominal concentration of 1 mg/ml. Before being tested, all stock solutions were bath-sonicated for 15 min and then aliquots were added first to 0.05 % (v/v) BSA/PBS and then to the cultures directly. In order to identify the most suitable NP concentrations to test we previously investigated the effect of a wide range of NP mass concentration on A549 cells viability by means of colony forming efficiency (CFE) assay. For this purpose, we treated the cells with NP concentrations ranging from 1.25 to 80 μg/cm^2, corresponding to a range of 8.3 to 266.6 μg/ml, an exposure range representative of realistic human exposure (Gangwal et al., 2011). In this way the concentrations of 10, 20 and 40 μg/cm^2 were selected for

genotoxicity studies, excluding the concentration of 80 μg/cm^2 since at this concentration NP caused a marked turbidity of the medium. For cellular uptake study, we chose the intermediate time and concentration used in genotoxicity investigations. We selected the 20 μg/cm^2 NP concentration to perform FISH analysis because this test concentration allowed us to prevent excessive particles deposition on the slides and interference during data acquisition. Since the 40 μg/cm^2 dose induced the maximum frequency of micronucleus (MN) this dose was used for the DNA methylation studies in order to observe if the genomic instability was correlated to global DNA methylation changes.

2.5. TiO_2 NP internalization

To study NP cell internalisation, A549 cells were seeded in 75 cm^2 flask (Corning Costar, Italy) at a density of 3x10^5 cells in 10 ml of complete cell culture medium. After 24 h, cells were exposed to 20 μg/cm^2 of TiO_2 NP for 48 h. After exposure, the medium was removed and cells were thoroughly washed with PBS buffer, detached using 1 ml trypsin-EDTA (Invitrogen, Italy) and centrifuged at 200xg for 5 min to obtain the cell pellet. The supernatant was removed and cells were fixed using a Karnovsky 2% v/v solution (glutaraldehyde and paraformaldehyde in 0.05 M cacodilate, pH 7.3, Sigma Aldrich, Italy) over night.

Cells were then washed 3 times with 0.05 M cacodilate pH 7.3 (Sigma Aldrich, Italy) and post-fixed in osmium tetroxide solution in 0.1 M cacodilate pH 7.3 (Sigma Aldrich, Italy) for 1 h. After 3 washes in cacodilate 0.05 M of 10 min each, cells were dehydrated in a graded series of ethanol solution in MilliQ water (30%; 50%; 75%; 95% for 15 min each, and 100% for 30 min), incubated in absolute propylene oxide (Sigma Aldrich, Italy) for 20 min (2 changes of 10 min each) and embedded in a solution of 1: 1 epoxy resin (Sigma Aldrich, Italy) and propylene oxide for 90 min. This mixture was renewed with pure epoxy resin (Sigma Aldrich, Italy) over night at room temperature and later polymerized at 60 °C for 48 h. Ultrathin sections (60-90 nm) were obtained using Leica UCT ultramicrotome (Leica, Italy) and stained for 25 min with uranyl acetate (Sigma

Aldrich, Italy) and lead citrate for 20 min, washed and dried. Ultrathin sections were imaged by JEOL JEM-2100 HR-transmission electron microscope at 120 kV.

The elemental analysis was carried in TEM mode at 120kV by Energy-dispersive X-ray spectroscopy (EDS) analysis using X-Flash Detector 5030 (Brüker, Italy) coupled with the microscope. Results are expressed as mass % of whole sample elements measured fixing at 0 the following elements: U, Pb, Os, Cu. Quantitative analysis of analysed area was automatically obtained by Cliff-Lorimer deconvoluted model using QUANTAX 200 software (Brüker, Italy).

2.6. Colony Forming Efficiency (CFE) assay

CFE assay was performed as detailed elsewhere (Ponti et al., 2013) to study the cytotoxicity induced by TiO_2 NP at 24, 48 and 72 h of exposure. Cells were seeded at the density of 300 cells per dish in 3 ml complete culture medium (60 × 15 mm Petri dish, 20 cm^2 bottom surface area, BD Falcon™). After 24 h, NP suspensions were directly added to the cell culture to obtain the appropriate final TiO_2 NP concentrations ranging from 1.25 to 80 μg/cm^2, corresponding to a range of 8.3‑266.6 μg/ml. Negative (untreated cells) and positive (Na_2CrO_4 1000 μM) controls were also included. After 24, 48 or 72 h of exposure, the medium was changed with fresh complete culture medium, and 7 days later, the cells were fixed with 3.7% (v/v) of formaldehyde solution (Sigma-Aldrich, Milan, Italy) in phosphate buffered saline (PBS) (1×) without calcium, magnesium and sodium bicarbonate (Gibco), and stained with 10% (v/v) Giemsa solution (Sigma-Aldrich) in ultrapure water. Colonies were manually scored under a stereomicroscope. The results are expressed as CFE (%) = [(average of treatment colonies/average of control colonies) × 100] and the corresponding standard error mean [SEM % = SD/√(number of treatments)].

2.7. Cytokinesis-block micronucleus cytome (CBMN-cyt) assay and fluorescence in situ hybridization (FISH)

CBMN-cyt was performed according to the procedure described by Di Bucchianico and coauthors (Di Bucchianico et al., 2013). A total of 7.5×10^4 cells were seeded in six-well cell culture plates (9.6 cm^2 bottom surface area, Falcon ™) and after 24 h of culture, the cells were exposed toTiO_2 NP at the concentrations of 10, 20 and 40 µg/cm^2, corresponding to 32, 64 and 128 µg/ml, respectively, for 48 h. Mitomycin C (0.1 µg/ml; MMC, Kyowa Hakko Kogyo Co, Chiyoda, Tokyo, Japan) as positive control was used. Cytochalasin B (6 µg/ml) was added after 44 h to block the cytokinesis process and cells were harvested after 72 h.

The parameters evaluated were the cytokinesis-block proliferation index (CBPI) and the replication index (RI) to test the cytostasis and the apoptotic and necrotic indices to investigate the cytotoxicity exerted by TiO_2 NP in the first 500 cells counted. These parameters were evaluated using the following formulas:

$$\text{CBPI} = \frac{((1 \text{ x mononucleate cells}) + (2 \text{ x binucleate cells}) + (3\text{x multinucleate cells}))}{500 \text{ cells}}$$

$$\text{RI} = \frac{((1 \text{ x mononucleate cells}) + (2 \text{ x multinucleate cells})) \div (500 \text{ treated cells})}{((1 \text{ x mononucleate cells}) + (2 \text{ x multinucleate cells})) \div (500 \text{ untreated cells})} \text{ x } 100$$

$$\text{Apoptotic index} = \frac{\text{Number of apoptotic cells}}{500 \text{ cells}} \text{ x } 100$$

$$\text{Necrotic index} = \frac{\text{Number of necrotic cells}}{500 \text{ cells}} \text{ x } 100$$

The genotoxic potential was evaluated by scoring the MN frequency on 1000 binucleated cells per slide. On these 1000 binucleated cells other parameters such as nucleoplasmic bridges (NPB), a biomarker of DNA misrepair and/or telomere end-fusions, and nuclear buds (NBUD), a biomarker of elimination of amplified DNA and/or DNA repair complexes, were also scored as previously described (Di Bucchianico et al., 2013; Fenech, 2007). Separate slides from CBMN Cyt were used to achieve FISH with human pancentromeric probes (Kreatech Diagnostics, Netherlands) as previously described (Di Bucchianico et al., 2013). Samples exposed for 48 hours to 20 μg/cm^2, and to positive (0.1 μg/ml MMC, clastogen) and negative controls, were classified as centromere positive (Cen+) or centromere negative (Cen-) based on the presence or on the absence of centromeres in MN.

2.8. Primary and oxidative DNA damage

Comet assay was performed to evaluate the primary and the oxidative DNA damage induced by TiO_2 NP in A549 cell cultures seeded at a concentration of 7×10^4 cells/cm^2 in six well cell culture plates (9.6 cm^2 bottom surface area, Falcon ™) by using the Comet Assay kit following the manufacturer's instructions (Trevigen, Gaithersburg, MD). After 24 h cells were treated with TiO_2 NP at 10, 20 and 40 μg/cm^2, corresponding to 32, 64 and 128 μg/ml respectively, for 48 h. To determine the presence of oxidized pyrimidine and purine bases Endonuclease III (EndoIII) and Formamidopyrimidine-DNA Glycosylase (Fpg) enzymes were used. To determine the number of enzyme-sensitive sites, the difference between the value of the percent DNA fluorescence in tail obtained after digestion with each enzyme and with the buffer only was calculated. The percentage of total DNA fluorescence in tail in a total of 100 randomly selected cells per sample (two replicates, each with 50 cells/slide) was used as a measure of the amount of primary DNA damage. Untreated cells (negative control) and cells exposed for 5 min to H_2O_2 (50 μM) as positive control were used. Three independent experiments were performed for each treatment by avoiding direct

light exposures of preparing slides. Analysis was carried out by using a Comet Image Analysis System, version 5.5 (Kinetic Imaging, Nottingham, UK).

2.9. Global DNA methylation analysis

Global DNA methylation was assessed using an ELISA method able to detect LINE-1 methylation degree, following the manufacturer's protocol (Active Motif, California USA). Briefly, genomic DNA was extracted using the QIAmp DNA blood Mini Kit (Qiagen, Milan,Italy, Catalog N° 51106). Cells were treated for 48 and 72 h with 40 µg/cm^2, corresponding to 128 µg/ml of NP and with 5-azacytidine (Sigma, MO, USA), a well-known demethylating agent, at the same treatment conditions. The extracted DNA was quantified using a Nano Drop ND 2000c spectrophotometer (NanoDrop Thermo scientific). 1 µg of DNA was enzymatically digested using the *MseI* enzyme in order to generate the appropriate fragmentation to hybridize to a biotynilated consensus sequence corresponding to human LINE-1 transposon. Hybridized samples were immobilized to a 96-well plate and methylated cytosines were identified using a 5-methylcytosine antibody, HRP-conjugated secondary antibody and colorimetric detection reagents. Generating a standard curve using DNA standards with known LINE-1 methylation levels, we were able to provide the relative level of 5-methylcyotsine in % of each DNA sample. To this purpose we used the ''polyfit'' interpolating function within program MatLab (The MathWorks, Inc., USA). Having obtained the interpolation curve of 7 DNA standards with a known methyaltion level (0, 10, 20, 30, 50, 75 and 100% of methylation), imputation of the absorbance reading (OD 450 nm, with an optimal reference wavelength of 655 nm) for each sample, yields a precise percentage of methylation of the template of interest. To perform the absorbance reading a Bio-Rad680 microplate reader (Bio-Rad, Italy) was used.

2.10. Statistical analysis

Data of toxicological assays derive from at least three independent experiments and are presented as the mean ± SEM. Since no difference was observed between negative and solvent control (ultrapure water) for NP, statistical analysis was performed only to evaluate differences between negative control and NP treated cells. The approach to test statistical significance of differences between negative control and NP-treated groups was one-way analysis of variance (ANOVA) followed by the Dunnett multiple comparison test. Linear regression equation was used to calculate the effect of mass concentration on each endpoint. Statistical analyses were carried out using GraphPad Prism 5 software. Results were considered statistically significant at $P< 0.05$.

3. Results

3.1. Characterization of NP

Data referred to colloidal characterization of pristine and modified samples in deionized water are reported in table 1.

→ Table 1

Citrate coated sample resulted the best-dispersed whilst P25 showed the highest agglomeration factor. The different values of Zeta potential recorded are in accordance with those expected with a reverse of TiO_2 positive Zeta potential value induced by anionic citrate modifier. The electrosteric stabilization induced by anionic organic coating is confirmed by the resulting lowest agglomeration factor. As reported in table 2, the results were compared with those obtained dispersing pristine and modified TiO_2 in complete culture medium Ham's F12. They evidenced the following behaviors:

- a dramatic destabilization of the system occurred for uncoated and silica coated samples. No strong effects were observed for citrate coated that maintained a good level of dispersion and P25 sample that showed the same degree of agglomeration as in deionized water.
- Zeta potential of all samples was leveled-off around -10/-20 mV, showing the slightly negative Z potential expected by BSA and other protein components at neutral pH (BSA isoelectric point ≅ 5) (Rezwan et al., 2005). These results suggest the presence of protein coating that masks TiO_2 NP surface charges, as explained by the well-known protein corona paradigm (Lynch et al., 2008). Similar trend was found in a previous work of ours, where the same uncoated and coated (citrated and silicated) TiO_2 NP were dispersed in complete culture medium MEM (Stoccoro et al., 2016).

→ Table 2

TiO_2 NP TEM imaging are reported in Figure 1. The first evidence arising by comparing different TiO_2 preparations with TiO_2 P25 is the thinner structure of TiO_2 nanosols primary particles (A) as obtained by wet chemical sol-gel process in comparison with P25 that is produced by high temperature flame hydrolysis synthesis (aerosol process, Evonik) (D). Moreover, in the silicated sample (B) a homogeneous dispersion of TiO_2 NP (mean diameter ~5nm) within SiO_2 matrix can be observed, confirming the formation of silica matrix encapsulated structure as previously reported (Ortelli et al., 2016) that is significantly different from the traditional core-shell structure. Finally, in the presence of the organic modifier (C), the very thin nano-structure of primary particles aggregate suggests the formation of NP clusters due to solvent evaporation during sample preparation.

→Figure 1

3.2. TiO_2 NP internalization in A549 cells

TEM analysis showed mostly single particle uptake for P25 (Figure 2 A-B), while for pristine, citrate and silica coated TiO_2 NP mainly NP agglomerates were found (Figure 2 C-D-E). All cells analyzed appeared with healthy cells morphology and no evident signs of cell damage were found after exposure to NP. Even if a large amount of TiO_2NP was present, cells maintained the ability to duplicate and survive. No apoptosis or cell necrosis were observed. TiO_2 NP were found both outside and inside cells where they were mostly localized in lysosomes, early and late endosomes. In the case of P25 the uptake was qualitatively (2-5% of total cells randomly analyzed) and quantitatively (0.4 mass % of total elements measured) lower than pristine (3.52 mass %), citrate (9.08 mass %) and silica coated (Ti: 1.78 mass %; Si: 6.11 mass %) (Figure 2 F) samples were 100% of cells randomly analyzed (e.g. 10 ultrafine slice cells/10 analyzed) showed NP internalization.

In the case of pristine, citrate and silica coated samples, large vacuoles containing NP were found suggesting active intracellular trafficking and cell metabolism, and no NP free in the cytoplasm were observed. Instead for P25 two main ways of uptake were observed: single particle internalization not associated to a specific mechanism (Figure 2A) and endo-phagocytic pathway (Figure 2B).

→Figure 2

3.3. Cell Viability

The cytotoxic potential of TiO_2 NP in A549 cells has been investigated by CFE assay (Figure 3). Cells were exposed to increasing concentrations (1.25 – 80 $\mu g/cm^2$) of TiO_2 NP for 24, 48 and 72 h. All NP induced a weak, although statistically significant, decrement in cell viability at all times of exposure. Pristine NP induced statistically significant cytotoxic effects at all the doses after 24 and

48 h of exposure, while after 72 h only the doses of 20, 40 and 80 µg/cm^2 induced significant effects (P<0.05, P<0.01 and P<0.001 respectively). Silica coated NP induced significant inhibitory effects at all the doses after 24 h of exposure, while after 48 h the 1.25 and 5 µg/cm^2 doses and after 72 h the 1.25 µg/cm^2 dose, induced slightly cytotoxic effects not statistically significant. Regarding the citrate coated NP, except for the lower concentration, after 24 h of treatment all the exposures induced statistically significant cytotoxic effects. P25 NP induced cytotoxicity at all the concentrations tested after 24 and 72 h of exposure, while following 48 h the 1.25 and 10 µg/cm^2 treatments did not induce significant effects.

→Figure 3

3.4. Cytostasis and cell death

CBPI and RI showed a cytostatic effect of both pristine and remediated TiO_2 NP on A549 cells compared to the untreated control cells. Apoptotic index values indicated that pristine NP and citrate coated NP were cytotoxic at all concentrations tested, while the silica coated NP induced apoptosis in a statistically significant manner only at 40 µg/cm^2. On the other hand, the Aeroxide® P25 did not induce apoptosis. Necrotic index values showed that only the citrate coated NP were able to induce cell death at all the concentrations tested, while the pristine NP at 20 and 40 µg/cm^2 and the silica coated and the Aeroxide® P25 at 40 µg/cm^2 induced necrosis.

→Figure 4

3.5. Chromosomal damage

Chromosomal damage was evaluated by scoring MN, NPB and NBUD frequencies in binucleated A549 cells (Figure 5). All the NP induced MN formation at all the NP concentrations tested, with

the exception of the silica coated NP at 10 μg/cm^2. The strongest MN induction was exerted by the highest exposure of the pristine NP (42.75 ± 1.89). Moreover, the induction of MN by pristine NP increased linearly with increasing concentrations (P=0.0162, R^2= 99.93). The genotoxic effects of the pristine NP were also demonstrated by the increased frequencies of NPB and of NBUD, which were induced by all the concentrations tested. Silica coated NP induced NPB at 20 and 40 μg/cm^2 while NBUD were found following all the exposures. Regarding the citrate coated NP, NPB were induced at all the concentrations tested, while the NBUD frequency increased only at the intermediate concentration. The Aeroxide® P25 induced the formation of NPB at all the concentrations tested, while no significant induction of NBUD was detected.

→Figure 5

In order to distinguish clastogenic and aneuploidogenic events, FISH analysis with pan-centromeric probes was performed (Figure 6). All TiO_2 NP exerted a weak aneuploidogenic activity compared to the untreated cells as evaluated by the presence of positive centromeric signals (37.5% Cen+). Aeroxide® P25 showed the highest value (45.5% Cen+) and pristine, silica and citrate coated NP induced a limited number of Cen+ (39.1%, 41.7%, 42.9% Cen+, respectively). However, these effects were not statistically significant.

→Figure 6

3.6. Primary and oxidative DNA damage

The DNA damage exerted by TiO_2 NP was evaluated by comet assay (Figure 7). Pristine NP induced a statistically significant primary DNA damage at 40 μg/cm^2. Silica coated NP did not induce primary DNA damage while the citrate coated NP induced statistically significant effects at

20 and 40 μg/cm^2. The Aeroxide P25 induced strong effects at all the concentrations tested with a linear DNA damage induction increasing along with concentrations (P = 0.019, R^2 =0.99). We also performed the comet assay with Endo III and Fpg enzymes in order to evaluate the induction of oxidatively damaged DNA by NP. From figure 7 it is noted that all NP were able to induce pyrymidine oxidative damage, whilst only the pristine, silica coated and P25 at 40 μg/cm^2 were able to induce purine oxidation.

→Figure 7

3.7. Global DNA methylation analysis

In Figure 8 are reported the effects of TiO_2 NP on global DNA methylation status in A549 cells after 48 and 72 h of treatment. We derived an interpolation curve using DNA standards of known methylated/unmethylated ratio (0%, 10%, 20%, 30%, 50%, 75%, and 100% of methylation) to obtain the best estimate of the extent of methylation for each of our samples. After 48 h of exposure TiO_2 NP did not affect the methylation degree of LINE-1 sequences. In fact the untreated cells showed a global DNA methylation level (%M) of 77.85%, and DNA of the cells treated with pristine, silica and citrate coated NP and with Aeroxide P25 showed a comparable methylation level (77.46, 77.52, 75.54 and 73.24 %M respectively). On the other hand, after 72 h of exposure all the NP tested induced a demethylation effect respect to the negative control (80.79%M) . The strongest effect was induced by the citrate coated NP (8.05%M, P<0.001), followed by the silica coated NP (21.67%M, P< 0.01) and Aeroxide P25 (34.15%M, P<0.05). Pristine NP showed the lower effect, (47.44%M), which is not statistically significant. As internal control of the experiment we used the 5-Azacytidine, a well known demethylating agent (Christman, 2002). In our experimental model 5-Azacytidine was able to induce a strong demethylating effect both after 48 hand 72 h (3.81%M and 11.71%M, respectively) of exposure.

→ Figure 8

4. Discussion

In this study the cytotoxic, genotoxic and epigenetic effects of uncoated anatase and TiO_2 NP engineered with silica and sodium citrate have been investigated in A549 cells. In order to better understand in which extent the remediation strategy adopted was able to mitigate the adverse effects induced by the pristine NP, several endpoints were analyzed. In table 3 a summary of the results obtained, by taking into account comparable conditions, is reported.

→Table 3

The coating with silica and citrate did not change the ability of pristine NP to enter the cells. In fact, both the pristine and the coated NP were observed into the cells contained in large vacuoles (Figure 2 C-D-E) suggesting mainly an endo-phagocytosis uptake mechanism. Characterization of TiO_2 NP uptake is critical to better understand modes of toxic action of NP. The ability of TiO_2 NP to enter A549 cells has already been reported (Ahlinder et al., 2013; Aueviriyavit et al., 2012; Janer et al., 2014; Jugan et al., 2012). In one of these studies the capacity of TiO_2 NP to internalize in A549 cells was investigated in living cells with a label free technique (Raman spectroscopy). TiO_2 NP were present in agglomerates inside vacuoles in the cytoplasm and after a NP deagglomeration, due to the acidic environment in the vicinity of lipid membranes, they entered in the nucleus, providing evidence of potential direct interactions between TiO_2 NP and DNA (Ahlinder et al., 2013).

A slight but statistically significant viability reduction evaluated by means of CFE assay and Cytome assay, were induced by all the NP tested and the NP remediation with silica and citrate coating did

not induce an improvement in NP safety (Figures 3 and 4). In particular, the presence of citrate increased the toxic effects induced by pristine NP as evaluated by RI and apoptotic and necrotic indices. Several papers are available in literature regarding cytotoxic effects of TiO_2 NP on A549 cells. Both no cytotoxic (Allegri et al., 2016; Chusuei et al., 2013; Ivask et al., 2015; Monteiller et al., 2007; Soto et al., 2008; Karlsson et al., 2008) and cytotoxic properties of TiO_2 NP (Jugan et al., 2012; Jin et al., 2014; Kansara et al., 2015) are reported. Several factors could lead to the different adverse effects of TiO_2 NP on A549 cell viability observed in the different studies, such as TiO_2 NP shape (Medina-Reyes et al., 2015) and the media used for cell culture (Gutierrez et al., 2015). In a recent paper TiO_2 NP resulted non-toxic in A549 cells grown in two-dimensional cultures but were able to affect cell-cell interaction during spheroid formation of A549 cells in three-dimensional cultures, as evaluated by means of fluorescent based method viability test (Sambale et al., 2015). These evidences highlight the need to consider all the experimental variables such as the viability assay used that could influence the results. In this context the CFE assay has been considered a suitable and robust *in vitro* method to assess cytotoxicity of NP by the European Commission's Joint Research Centre (JRC) (Ponti et al., 2014).

Genotoxicity, evaluated by means of micronuclei, NPB and NBUD scoring, was induced by all NP tested (Figure 5). It is known that A549 is not one of the cell lines extensively validated for micronucleus testing. However we chose human lung alveolar epithelial cells (A549), as a model system for the potential inhalation health effects, frequently used in nanotoxicity studies (Love et al., 2012).

Several researchers investigated TiO_2 NP genotoxicity in A549 cells by means of MN assay, however conflicting results were often found. In fact, both negative (Jugan et al., 2012; Dhasmana et al., 2014; Armand et al., 2016) and positive (Kansara et al., 2015; Srivastava et al., 2011) capacity to induce micronuclei were observed. These conflicting results could be due to the differences in physicochemical properties of TiO_2 NP suspensions, such as different NP sizes, crystalline phase, specific surface area, that can influence the interaction of NP with the cell

medium and then NP agglomeration status, which is considered an important factor to take into account in order to improve the quality of the CBMN-cyt assay (Migliore et al., 2014). In order to investigate if the micronuclei induction had a clastogenic or an aneuploidogenic origin we performed a FISH analysis on treated cells. FISH results showed that all TiO_2 NP tested induced mainly clastogenic damage and enhanced slightly, but in a non-statistically significant manner, centromere positive micronuclei compared to the untreated cells (Figure 6). Few studies regarding clastogenic and aneuploidogenic effects induced by NP by means of FISH analysis are available in literature. In our laboratory it was observed that 5 and 15 nm Au NP induced aneuploidy in human primary lymphocytes and in murine macrophages (Di Bucchianico et al., 2014). Aneuploidogenic properties were also observed for cobalt chrome (CoCr) NP (Raghunathan et al., 2013). Clastogenic properties were observed for Au NP (Li et al., 2011a), while both clastogenic and aneuploidogenic activity were observed for MWCNT (Muller et al., 2008) and for silica NP (Gonzalez et al., 2010). Regarding TiO_2 NP Rahman and collaborators observed that TiO_2 NP with a mean size <20 nm induced formation of micronuclei in Syrian hamster embryo (SHE) cells, and kinetochore analysis revealed that MN mainly arise from clastogenic events (Rahman et al., 2002), thus supporting our observations.

DNA damage investigation, evaluated by means of comet assay, showed that the presence of citrate increased the genotoxic effects of the pristine NP, while the silica coated NP induced effects comparable to that of uncoated ones. The strongest effects were induced by P25 (Figure 7). DNA oxidation experiments showed that all NP induced oxidative DNA damage, although only the concentration of 40 $\mu g/cm^2$ of pristine, silica coated and P25 NP induced statistically significant effects ($P<0.05$).

Our results are supported by several research papers in which the capacity of TiO_2 NP to induce both primary and oxidative DNA lesions in A549 cells was investigated by means of comet assay (Jugan et al., 2012; Karlsson et al., 2008; Kansara et al., 2015; Armand et al., 2016; Ursini et al.,

2014; Wang et al., 2015). These studies clearly indicate that TiO_2 NP are able to induce DNA breakage and oxidative damage to DNA of A549 cells.

Since DNA hypomethylation has been associated with genomic instability, and in particular with the formation of micronuclei (Luzhna et al., 2013), we investigated global DNA methylation in treated cells in order to observe whether there was any correlation with MN formation. After 48 h of exposure the tested NP did not induce effects on LINE-1 methylation, while after 72 h of exposure a significant demethylating effect was induced by the silica and the citrate coated NP, the latest inducing the strongest effects (Figure 8). The time of exposure had a pivotal role in establishing changes in DNA methylation levels. Thus the MN induction, evaluated after a treatment of 48 h, did not seem to be correlated to global DNA hypomethylation. Global DNA hypomethylation induces mainly genomic instability of aneuploidogenic origin (Cho et al., 2015) and results from FISH analysis indicate that the MN induction is mainly of clastogenic origin, further suggesting that DNA methylation likely does not have a role in TiO_2 NP MN formation.

LINE-1 methylation analysis is frequently used in epigenetic investigations as a surrogate for global DNA methylation levels of the cells and can be utilized to compare relative changes in 5-methylcytosine (5-mC) across different samples and treatment conditions. This comparison correlates well with total 5-mC content when compared to other techniques such as high performance liquid chromatography (HPLC) or combined bisulfite restriction analysis (COBRA) and pyrosequencing (Yang et al., 2004; Weisenberger et al., 2005). LINE-1 hypomethylation has been associated with elevated risk of several disease states including cancer, stroke, heart disease, lung function decline and it has also been considered a prognostic factor in gliomas (Ogino et al., 2008; Cho et al., 2009; Baccarelli et al., 2010; Lange et al., 2012; Ohka et al., 2011). Moreover LINE-1 hypomethylation was observed in peripheral blood DNA cells of subjects exposed to ultrafine particles (Baccarelli et al., 2009; Madrigano et al., 2011).

Several studies were performed so far to evaluate NP potential epigenetic properties. For instance *in vitro* experiments showed that, SiO_2 NP induced DNA hypomethylation (Gong et al., 2010; Gong et

al., 2012), cadmium telluride quantum dots (CdTeQDs) induced global hypoacetylation (Choi et al., 2008) and Au NP and CdTeQDs induced deregulation of miRNA expression (Li et al., 2011b; Ng et al., 2011). Regarding epigenetic effects of TiO_2 NP, the few studies reported in literature indicate that TiO_2 NP are able to induce altered miRNA expression and DNA methylation impairment. In lung of mice, the inhalation of surface-coated with polyalcohol TiO_2 NP induced changes in the expression of genes associated with acute phase, inflammation and immune response with concomitant changes in the expression of several miRNAs (Halappanavar et al., 2011). Treatment of HaCaT cells with TiO_2 NP led to several significant biochemical changes among which dysfunction of the methionine cycle and methionine deficiency, suggesting an impairment in DNA methylation reactions of the cells after TiO_2 NP exposure (Tucci et al., 2013). TiO_2 NP induced aberrant hypermethylation of poly(ADP-ribose) polymerase 1(*PARP-1*) gene, that encode a protein involved in DNA repair, in cell proliferation and in chromatin modification, in A549 cells treated for 24 h with concomitant increase of ROS (Bai et al., 2015). In a recent study both human and murine macrophages were exposed to several nanomaterials, including TiO_2 NP and the effects of the treatment on global DNA methylation were evaluated (Lu et al., 2015). In cells treated with 0.5 and 30 μg/ml of TiO_2 NP for 24 h a decreased expression of DNA methylation machinery was observed, without a significant difference of LINE1 methylation pattern between no exposed and exposed cells. These results could be explained by the short post-exposure time when a sufficient number of cell divisions had not yet occurred to detect potential alterations in DNA methylation (Lu et al., 2015).

Therefore both genotoxicity and epigenotoxicity could be driven by the well established capacity of TiO_2 NP to induce ROS formation, that could act as the primary event in promoting TiO_2 NP toxic effects.

Modification of NP surface by means of coating procedures influences the activity of NP, by changing their physicochemical properties. These modifications are aimed both to ameliorate the chemico-physical characteristics of NP and to decrease their potential toxicity. For example, the

coating of TiO_2 NP with a thiol-ene click chemistry and catalytic chain transfer polymerization induced stable NP aggregates in various aqueous and biological media changing the NP cellular uptake with a concomitant reduction of cytotoxicity in A549 human lung cells (Tedja et al., 2012).

As already stated, the remediation strategy adopted in the current study did not modify significantly cytotoxic and genotoxic properties of pristine TiO_2 NP, however these types of coating seem able to interfere with the global DNA demethylation effect of pristine NP. Until now few studies aimed to investigate the capacity of silica coating of TiO_2 NP have been carried out *in vivo* and in *in vitro*, showing both increase or reduction of the toxicity of the uncoated TiO_2 NP (Bolis et al., 2012; Feng et al., 2013; Rossi et al., 2010; Warheit et al., 2007). In a recent paper by us the genotoxicity and the capacity to induce morphological neoplastic transformation in murine cells by the same TiO_2 NP used in the current study were evaluated (Stoccoro et al., 2016). Also in that study we observed that the remediation strategy with silica and citrate did not improve the safety of uncoated NP, but instead the citrate coating increased the toxic effects of the pristine one. In particular, the coating with citrate conferred the capacity to the cells to undergo transformation. By analyzing the previous and present data it is evident that TiO_2 NP coated with citrate resulted more effective regarding the various toxic endpoints investigated (cytotoxicity, genotoxicity and epigenotoxicity).. It should be considered that the effects observed by citrate coated NP may be due in part by the coating itself rather than by NP. In a recent paper it was observed that silver NP (Ag NP) coated with trisodium citrate induced *HPRT* gene mutations in V79-4 cells (Huk et al., 2015). Interestingly sodium citrate alone was able to induce mutations analogously to those induced by Ag NP coated with citrate. Similarly, Wang and coworkers observed that gold NP coated with citrate were photomutagenic to *Salmonella typhimurium* TA 102, and further investigations revealed that the mutagenicity properties mainly derived from citrate and Au^{3+} ions (Wang et al., 2011).

In conclusion our results confirm that the TiO_2 NP investigated are able to induce genotoxicity, and epigenotoxicity. The presence of citrate results in an increase of pristine NP toxicological effect, suggesting an active role by the citrate itself, as elsewhere reported (Huk et al., 2015; Wang et al.,

2011), whilst the presence of silica does not seem significantly affect the toxic properties of uncoated NP (table 2).

It is well established that to better characterize the potential adverse effects of NP it is necessary to investigate their toxicological capacities in different model systems and by means of multiple genotoxic assays. In this context we consider it worthwhile to include assays that provide also information on induced epigenetic effects, as in recent years several investigations have shown that NP are able to induce aberrant epigenetic modifications (Shyamasundar et al., 2015). It is known that these mechanisms could indeed promote the onset of several types of diseases. Genotoxic and epigenotoxic mechanisms could work in association in the induction of adverse health effects and are able to benefit from each other (You and Jones, 2012; Sadikovic et al., 2012). In fact, genetic modifications in epigenetic regulators lead to epigenetic changes such as aberrant DNA methylation, histone modifications, and miRNA altered expression as well as modifications in epigenetic mechanisms can lead to genetic modifications, inducing genome instability and deregulation of crucial genes (Lengauer et al., 1997; You and Jones, 2012). So it would be desirable that future investigations that will be aimed at investigate the potential genotoxic mechanisms of NP, will be implemented also by investigations regarding their potentiality in inducing epigenetic modifications, in order to better understand the possible harmful effects of these nanomaterials.

Funding

This work was financially supported by the FP7 projects No 280716, SANOWORK.

Acknowledgments

We would like to thank Dr. Paolo Lucchesi (Department of Clinical and Experimental Medicine, University of Pisa) for assistance with TEM images acquisition.

References

Ahlinder, L., Ekstrand-Hammarström, B., Geladi, P. and Osterlund, L. (2013) Large uptake of titania and iron oxide nanoparticles in the nucleus of lung epithelial cells as measured by Raman imaging and multivariate classification. Biophys. J., 105(2):310-9. doi: 10.1016/j.bpj.2013.06.017.

Aitken, R.J., Chaudhry, M.Q., Boxall, A.B. and Hull, M. (2006) Manufacture and use of nanomaterials: current status in the UK and global trends. Occup. Med. (Lond), 56: 300-306.

Allegri, M., Bianchi., M.G., Chiu, M., Varet, J., Costa, A.L., Ortelli, S., Blosi, M., Bussolati, O., Poland, C.A. and Bergamaschi, E. (2016) Shape-Related Toxicity of Titanium Dioxide Nanofibres. PLoS One, 21;11(3):e0151365. doi: 10.1371/journal.pone.0151365.

Armand, L., Tarantini, A., Beal, D., Biola-Clier, M., Bobyk, L., Sorieul, S., Pernet-Gallay, K., Marie-Desvergne, C., Lynch, I., Herlin-Boime, N. and Carriere, M. (2016) Long-term exposure of A549 cells to titanium dioxide nanoparticles induces DNA damage and sensitizes cells towards genotoxic agents. Nanotoxicology, 22:1-11.

Aueviriyavit, S., Phummiratch, D., Kulthong, K. and Maniratanachote, R., 2012. Titanium dioxide nanoparticles-mediated in vitro cytotoxicity does not induce Hsp70 and Grp78 expression in human bronchial epithelial A549 cells. Biol. Trace. Elem. Res., 149(1):123-32. doi: 10.1007/s12011-012-9403-z.

Baccarelli, A., Wright, R., Bollati, V., Litonjua, A., Zanobetti, A., Tarantini, L., Sparrow, D., Vokonas, P. and Schwartz, J. (2010) Ischemic heart disease and stroke in relation to blood DNA methylation. Epidemiology, 21(6):819-28. doi: 10.1097/EDE.0b013e3181f20457.

Baccarelli, A., Wright, R.O., Bollati, V., Tarantini, L., Litonjua, A.A., Suh, H.H., Zanobetti, A., Sparrow, D., Vokonas, P.S. and Schwartz, J. (2009) Rapid DNA methylation changes after exposure to traffic particles. Am. J. Respir. Crit. Care Med., 1;179(7):572-8. doi: 10.1164/rccm.200807-1097OC.

Bai, W., Chen, Y. and Gao, A. (2015) Cross talk between poly(ADP-ribose) polymerase 1 methylation and oxidative stress involved in the toxic effect of anatase titanium dioxide nanoparticles. Int. J. Nanomedicine, 1;10:5561-9. doi: 10.2147/IJN.S88059.

Bolis, V., Busco, C., Ciarletta, M., Distasi, C., Erriquez, J., Fenoglio, I., Livraghi, S. and Morel, S. (2012) Hydrophilic/hydrophobic features of TiO2 nanoparticles as a function of crystal phase, surface area and coating, in relation to their potential toxicity in peripheral nervous system. J. Colloid. Interface Sci., 369, 28–39.

Chen, T., J. Yan, and Y. Li. (2014) Genotoxicity of titanium dioxide nanoparticles. J. Food. Drug Anal., 22: 95-104.

Cho, N.Y., Kim, J.H., Moon, K.C. and Kang, G.H. (2009) Genomic hypomethylation and CpG island hypermethylation in prostatic intraepithelial neoplasm. Virchows Arch., 454(1):17-23. doi: 10.1007/s00428-008-0706-6.

Cho, Y.H., Woo, H.D., Jang, Y., Porter, V., Christensen, S., Hamilton, R.F. Jr and Chung, H.W. (2015) The Association of LINE-1 Hypomethylation with Age and Centromere Positive Micronuclei in Human Lymphocytes. PLoS One, 21;10(7):e0133909. doi: 10.1371/journal.pone.0133909.

Choi, A.O., Brown, S.E., Szyf, M., Maysinger D. (2008) Quantum dot-induced epigenetic and genotoxic changes in human breast cancer cells. J Mol Med (Berl), 86(3):291-302.

Christman, J.K. (2002) 5-Azacytidine and 5-aza-2'-deoxycytidine as inhibitors of DNA methylation: mechanistic studies and their implications for cancer therapy. Oncogene, 12;21(35):5483-95

Chusuei, C.C., Wu, C.H., Mallavarapu, S., Hou, F.Y., Hsu, C.M., Winiarz, J.G., Aronstam, R.S., and Huang, Y.W. (2013) Cytotoxicity in the age of nano: the role of fourth period transition metal oxide nanoparticle physicochemical properties. Chem. Biol. Interact., 206: 319-326.

Dhasmana, A., Sajid Jamal, Q.M., Mir, S.S., Bhatt, M.L., Rahman, Q., Gupta, R., Siddiqui, M.H. and Lohani, M. (2014) Titanium dioxide nanoparticles as guardian against environmental carcinogen benzo[alpha]pyrene. PLoS One, 12;9(9):e107068. doi: 10.1371/journal.pone.0107068.

Di Bucchianico, S., Fabbrizi, M.R., Cirillo, S., Uboldi, C., Gilliland, D., Valsami-Jones, E. and Migliore L. (2014) Aneuploidogenic effects and DNA oxidation induced in vitro by differently sized gold nanoparticles. Int. J. Nanomedicine, 8;9:2191-204. doi: 10.2147/IJN.S58397.

Di Bucchianico, S., Fabbrizi, M.R., Misra, S.K., Valsami-Jones, E., Berhanu, D., Reip, P., Bergamaschi, E. and Migliore, L. (2013) Multiple cytotoxic and genotoxic effects induced in vitro by differently shaped copperoxide nanomaterials. Mutagenesis, 28, 287–299.

Fenech, M. (2007) Cytokinesis-block micronucleus cytome assay. Nat. Protoc., 2, 1084–1104.

Feng, X., Zhang, S. and Lou, X. (2013) Controlling silica coating thickness on TiO2 nanoparticles for effective photodynamic therapy. Colloids Surf. B. Biointerfaces, 107, 220–226.

Gangwal, S., Brown, J. S., Wang, A., Houck, K. A., Dix, D. J., Kavlock, R. J. and Hubal, E. A. (2011) Informing selection of nanomaterial concentrations for ToxCast in vitro testing based on occupational exposure potential. Environ. Health Perspect., 119, 1539–1546.

Gong, C., G. Tao, L. Yang, J. Liu, Q. Liu and Z. Zhuang. (2010) SiO(2) nanoparticles induce global genomic hypomethylation in HaCaT cells. Biochem. Biophys. Res. Commun., 397: 397-400.

Gong, C., G. Tao, L. Yang, J. Liu, Q. Liu, W. Li and Z. Zhuang. (2012) Methylation of PARP-1 promoter involved in the regulation of nano-SiO2-induced decrease of PARP-1 mRNA expression. Toxicol. Lett., 209: 264-269.

Gonzalez, L., Thomassen, L.C., Plas, G., Rabolli, V., Napierska, D., Decordier, I., Roelants, M., Hoet, P.H., Kirschhock, C.E., Martens, J.A., Lison, D. and Kirsch-Volders, M. (2010) Exploring the aneugenic and clastogenic potential in the nanosize range: A549 human lung carcinoma cells and amorphous monodisperse silica nanoparticles as models. Nanotoxicology, 4:382-95. doi: 10.3109/17435390.2010.501913.

Gutierrez, E. R., Kamens, R. M., Tolocka, M., Sexton, K. and Jaspers, I. (2015) A comparison of three dispersion media on the physicochemical and toxicological behavior of TiO2 and NiO nanoparticles. Chem. Biol. Interact., 236: 74-81.

Halappanavar, S., Jackson, P., Williams, A., Jensen, K. A., Hougaard, K. S., Vogel, U., Yauk, C. L. and Wallin, H. (2011) Pulmonary response to surface-coated nanotitanium dioxide particles includes induction of acute phase response genes, inflammatory cascades, and changes in microRNAs: a toxicogenomic study. Environ. Mol. Mutagen., 52: 425-439.

Huk, A., Izak-Nau, E., El Yamani, N., Uggerud, H., Vadset, M., Zasonska, B., Duschl, A. Dusinska, M. (2015) Impact of nanosilver on various DNA lesions and HPRT gene mutations - effects of charge and surface coating. Part. Fibre Toxicol., 24, 12–25.

IARC, (2010) IARC monographs on the evaluation of carcinogenic risks to humans: carbon black, titanium dioxide, and talc. Lyon Fr. World Health Organ. Int. Agency Res. Cancer 93..

Ivask, A., Titma, T., Visnapuu, M., Vija, H., Kakinen, A., Sihtmae, M., Pokhrel, S., Madler, L., Heinlaan, M., Kisand, V., Shimmo, R. and Kahru, A., (2015) Toxicity of 11 Metal Oxide Nanoparticles to Three Mammalian Cell Types In Vitro. Curr. Top. Med. Chem., 15: 1914-1929.

Janer, G., Mas del Molino E., Fernández-Rosas, E., Fernández, A. and Vázquez-Campos, S. (2014) Cell uptake and oral absorption of titanium dioxide nanoparticles. Toxicol. Lett., 15;228(2):103-10. doi: 10.1016/j.toxlet.2014.04.014.

Jin, C., Wang, F., Tang, Y., Zhang, X., Wang, J., Yang, Y., 2014. Distribution of graphene oxide and TiO2-graphene oxide composite in A549 cells. Biol. Trace Elem. Res., 159: 393-398.

Jugan, M.L., Barillet, S., Simon-Deckers, A., Herlin-Boime, N., Sauvaigo, S., Douki, T. and Carriere, M. (2012) Titanium dioxide nanoparticles exhibit genotoxicity and impair DNA repair activity in A549 cells. Nanotoxicology, 6: 501-513.

Kansara, K., Patel, P., Shah, D., Shukla, R. K., Singh, S., Kumar, A. and Dhawan, A. (2015) TiO2 nanoparticles induce DNA double strand breaks and cell cycle arrest in human alveolar cells. Environ. Mol. Mutagen., 56: 204-217.

Karlsson, H.L., Cronholm, P., Gustafsson, J. and Moller, L. (2008) Copper oxide nanoparticles are highly toxic: a comparison between metal oxide nanoparticles and carbon nanotubes. Chem. Res. Toxicol., 21:1726-1732.

Lange, N.E., Sordillo, J., Tarantini, L., Bollati, V., Sparrow, D., Vokonas, P., Zanobetti, A., Schwartz, J., Baccarelli, A., Litonjua, A.A. and Demeo, D.L. (2012) Alu and LINE-1 methylation and lung function in the normative ageing study. BMJ Open, 17;2(5). pii: e001231. doi: 10.1136/bmjopen-2012-001231.

Lengauer, C., Kinzler, K.W. and Vogelstein, B. (1997) DNA methylation and genetic instability in colorectal cancer cells. Proc. Natl. Acad. Sci. U S A, 94: 2545-2550.

Li, J.J., Lo, S.L., Ng, C.T., Gurung, R.L., Hartono, D., Hande, M.P., Ong, C.N., Bay, B.H. and Yung, L.Y. (2011a) Genomic instability of gold nanoparticle treated human lung fibroblast cells. Biomaterials. 32(23):5515-23. doi: 10.1016/j.biomaterials.2011.04.023.

Li, S., Wang, Y., Wang, H., Bai, Y., Liang, G., Huang, N. and Xiao, Z. (2011b) MicroRNAs as participants in cytotoxicity of CdTe quantum dots in NIH/3T3 cells. Biomaterials, 32:3807-3814.

Love, S.A., Maurer-Jones, M.A., Thompson, J.W., Lin, Y.S. and Haynes, C.L. (2012) Assessing nanoparticle toxicity. Annu. Rev. Anal. Chem .(Palo Alto Calif), 5:181-205. doi: 10.1146/annurev-anchem-062011-143134.

Lu, X., Miousse, I.R., Pirela, S.V., Melnyk, S., Koturbash, I. and Demokritou, P. (2015) Short-term exposure to engineered nanomaterials affects cellular epigenome. Nanotoxicology, 4:1–11.

Luzhna, L., Kathiria, P. and Kovalchuk, O. (2013) Micronuclei in genotoxicity assessment: from genetics to epigenetics and beyond. Front. Genet., 4:131. doi: 10.3389/fgene.2013.00131.

Lynch, I. and Dawson, K.A. (2008) Protein-nanoparticle interactions. Nanotoday, 3:40–47.

Madrigano, J., Baccarelli, A., Mittleman, M.A., Wright, R.O., Sparrow, D., Vokonas, P.S., Tarantini, L. and Schwartz, J. (2011) Prolonged exposure to particulate pollution, genes associated with glutathione pathways, and DNA methylation in a cohort of older men. Environ. Health Perspect., 119(7):977-82. doi: 10.1289/ehp.1002773.

Medina-Reyes, E. I., A. Deciga-Alcaraz, V. Freyre-Fonseca, N. L. Delgado-Buenrostro, J. O. Flores-Flores, G. F. Gutierrez-Lopez, Y. Sanchez-Perez, C. M. Garcia-Cuellar, J. Pedraza-Chaverri and Chirino, Y. I. (2015) Titanium dioxide nanoparticles induce an adaptive inflammatory response and invasion and proliferation of lung epithelial cells in chorioallantoic membrane. Environ. Res., 136: 424-434.

Migliore, L, Uboldi, C. and Di Bucchianico, S. (2014) The In Vitro Micronucleus Assay and FISH Analysis. Book Title: Genotoxicity and DNA Repair : A Practical Approach. Springer. Page Range: 73-102. DOI: 10.1007/978-1-4939-1068-7_5

Monteiller, C., L. Tran, W. MacNee, S. Faux, A. Jones, B. Miller, and K. Donaldson. (2007) The pro-inflammatory effects of low-toxicity low-solubility particles, nanoparticles and fine particles, on epithelial cells in vitro: the role of surface area. Occup. Environ. Med., 64:609-615.

Morimoto, Y., Izumi, H., Yoshiura, Y., Tomonaga, T., Lee, B.W., Okada, T., Oyabu, T., Myojo, T., Kawai, K,, Yatera, K., Shimada, M., Kubo, M., Yamamoto, K., Kitajima, S., Kuroda, E., Horie, M., Kawaguchi, K. and Sasaki, T. (2016) Comparison of pulmonary inflammatory responses following intratracheal instillation and inhalation of nanoparticles. Nanotoxicology, 10(5):607-18. doi: 10.3109/17435390.2015.1104740.

Muller, J., Decordier, I., Hoet, P.H., Lombaert, N., Thomassen, L., Huaux, F., Lison, D. and Kirsch-Volders, M. (2008) Clastogenic and aneugenic effects of multi-wall carbon nanotubes in epithelial cells. Carcinogenesis, 29(2):427-33. doi: 10.1093/carcin/bgm243.

Nel, A.E., Mädler, L., Velegol, D., Xia, T., Hoek, E.M., Somasundaran, P., Klaessig, F., Castranova, V., Thompson, M., 2009. Understanding biophysicochemical interactions at the nano-bio interface. Nat. Mater. 8,543–557.

Ng, C.T., Dheen, S.T., Yip, W.C., Ong, C.N., Bay, B.H. and Lanry Yung, L.Y. (2011) The induction of epigenetic regulation of PROS1 gene in lung fibroblasts by gold nanoparticles and implications for potential lung injury. Biomaterials, 32:7609-7615.

Ogino, S., Nosho, K., Kirkner, G.J., Kawasaki, T., Chan, A.T., Schernhammer, E.S., Giovannucci E.L. and Fuchs, C.S. (2008) A cohort study of tumoral LINE-1 hypomethylation and prognosis in colon cancer. J. Natl. Cancer Inst., 3;100(23):1734-8. doi: 10.1093/jnci/djn359.

Ohka, F., Natsume, A., Motomura, K., Kishida, Y., Kondo, Y., Abe, T., Nakasu, Y., Namba, H., Wakai, K., Fukui, T., Momota, H., Iwami, K., Kinjo, S., Ito, M., Fujii, M. and Wakabayashi, T. (2011) The global DNA methylation surrogate LINE-1 methylation is correlated with MGMT promoter methylation and is a better prognostic factor for glioma. PLoS One, 6(8):e23332. doi: 10.1371/journal.pone.0023332.

Ortelli, S. and Costa, A.L. (2016) Nanoencapsulation techniques as a “safer by (molecular) design” tool. Nano-Structures & Nano-Objects, Article in press. doi:10.1016/j.nanoso.2016.03.006

Ortelli, S., Blosi, M., Albonetti, S., Vaccari, A., Dondi, M. and Costa, A.L (2013) TiO2 based nano-photocatalysis immobilized on cellulose substrates. J. Photochem. Photobiol. A: Chem., 276,58‑64.

Ponti, J., Broggi, F., Mariani, V., De Marzi, L., Colognato, R., Marmorato, P., Gioria, S., Gilliland, D., Pascual Garcìa, C., Meschini, S., Stringaro, A., Molinari, A., Rauscher, H. and Rossi, F. (2013) Morphological transformation induced by multiwall carbon nanotubes on Balb/3T3 cell model as an in vitro end point of carcinogenic potential. Nanotoxicology, 7, 221‑233.

Ponti, J., Kinsner-Ovaskainen, A., Norlén, H. Altmeyer, S., et al., (2014) Interlaboratory comparison study of the colony forming efficiency assay for assessing cytotoxicity of nanomaterials. EUR.

Raghunathan, V.K., Devey, M., Hawkins, S., Hails, L., Davis, S.A., Mann, S., Chang, I.T., Ingham, E., Malhas, A., Vaux, D.J., Lane, J.D. and Case, C.P. (2013) Influence of particle size and reactive oxygen species on cobalt chrome nanoparticle-mediated genotoxicity. Biomaterials, 34(14):3559-70. doi: 10.1016/j.biomaterials.2013.01.085.

Rahman, Q., Lohani, M., Dopp, E., Pemsel, H., Jonas, L., Weiss, D.G. and Schiffmann, D. (2002) Evidence that ultrafine titanium dioxide induces micronuclei and apoptosis in Syrian hamster embryo fibroblasts. Environ. Health. Perspect., 110(8):797-800.

Rezwan, K., Studart, A. R., Vörös, J. and Gauckler, L. J. (2005) Change of zeta potential of biocompatible colloidal oxide particles upon adsorption of bovine serum albumin and lysozyme. J. Phys. Chem. B, 109,14469–14474.

Rossi, E.M., Pylkkänen, L., Koivisto, A. J., et al., (2010) Airway exposure to silica-coated TiO2 nanoparticles induces pulmonary neutrophilia in mice. Toxicol. Sci., 113, 422–433.

Sadikovic, B., Al-Romaih, K., Squire, J.A. and Zielenska, M. (2008) Cause and consequences of genetic and epigenetic alterations in human cancer. Curr. Genomics, 9:394-408.

Sambale, F., Lavrentieva, A., Stahl, F., Blume, C., Stiesch, M., Kasper, C., Bahnemann, D. and Scheper, T. (2015) Three dimensional spheroid cell culture for nanoparticle safety testing. J. Biotechnol., 10;205:120-9. doi: 10.1016/j.jbiotec.2015.01.001.

Shi, H., Magaye, R., Castranova, V., Zhao, J. (2013) Titanium dioxide nanoparticles: a review of current toxicological data. Part. Fibre Toxicol., 10: 15.

Shyamasundar, S., Ng, C.T., Yung, L.Y., Dheen, S.T. and Bay, B.H. (2015) Epigenetic mechanisms in nanomaterial-induced toxicity. Epigenomics, 7(3):395-411. doi: 10.2217/epi.15.3.

Soto, K.F., Murr, L. E. and Garza, K.M. (2008) Cytotoxic responses and potential respiratory health effects of carbon and carbonaceous nanoparticulates in the Paso del Norte airshed environment. Int. J. Environ. Res. Public Health, 5:12-25.

Srivastava, R.K., Rahman, Q., Kashyap, M.P., Lohani, M. and Pant, A.B. (2011) Ameliorative effects of dimetylthiourea and N-acetylcysteine on nanoparticles induced cyto-genotoxicity in human lung cancer cells-A549. PLoS One, 6(9):e25767. doi: 10.1371/journal.pone.0025767.

Stoccoro, A., Di Bucchianico, S., Uboldi, C., Coppedè, F., Ponti, J., Placidi, C., Blosi, M., Ortelli, S., Costa, A.L. and Migliore, L. (2016) A panel of in vitro tests to evaluate genotoxic and morphological neoplastic transformation potential on Balb/3T3 cells by pristine and remediated titania and zirconia nanoparticles. Mutagenesis. pii: gew015.

Stoccoro, A., Karlsson, H.L., Coppede, F. and Migliore, L. (2013) Epigenetic effects of nano-sized materials. Toxicology, 313:3-14. doi: 10.1016/j.tox.2012.12.002

Suzuki, T., Miura, N., Hojo, R., Yanagiba, Y., Suda, M., Hasegawa, T., Miyagawa, M. and Wang, R.S. (2016) Genotoxicity assessment of intravenously injected titanium dioxide nanoparticles in gpt delta transgenic mice. Mutat. Res. Genet. Toxicol. Environ. Mutagen., 802:30-7. doi: 10.1016/j.mrgentox.2016.03.007

Tedja, R., Soeriyadi, A.H., Whittaker M.R., Lim, M.C. Marquis, C. Boyer, Davis, T.P. and Amal, R. (2012) Effect of TiO2 nanoparticle surface functionalization on protein adsorption, cellular uptake and cytotoxicity: the attachment of PEG comb polymers using catalytic chain transfer and thiol–ene chemistry. Polymer Chemistry, 3:2743-2751.

Tucci, P., Porta, G., Agostini, M., Dinsdale, D., Iavicoli, I., Cain, K., Finazzi-Agró, A., Melino, G. and Willis, A. (2013) Metabolic effects of TiO2 nanoparticles, a common component of sunscreens and cosmetics, on human keratinocytes. Cell Death Dis., 21;4:e549. doi: 10.1038/cddis.2013.76.

Ursini, C.L., Cavallo, D., Fresegna, A.M., Ciervo, A., Maiello, R., Tassone, P., Buresti, G., Casciardi, S. and Iavicoli, S. (2014) Evaluation of cytotoxic, genotoxic and inflammatory response in human alveolar and bronchial epithelial cells exposed to titanium dioxide nanoparticles. J. Appl. Toxicol., 34(11):1209-19. doi: 10.1002/jat.3038.

Wang, Y., Cui, H., Zhou, J., Li, F., Wang, J., Chen, M. and Liu, Q. (2015) Cytotoxicity, DNA damage, and apoptosis induced by titanium dioxide nanoparticles in human non-small cell lung cancer A549 cells. Environ. Sci. Pollut. Res. Int., 22(7):5519-30. doi: 10.1007/s11356-014-3717-7.

Wang, S., Lawson, R., Ray, P.C. and Yu, H. (2011) Toxic effects of gold nanoparticles on Salmonella typhimurium bacteria. Toxicol. Ind. Health, 27(6):547-54. doi: 10.1177/0748233710393395.

Warheit, D.B., Webb, T.R., Reed, K.L., Frerichs, S. and Sayes, C.M. (2007) Pulmonary toxicity study in rats with three forms of ultrafine-TiO2 particles: differential responses related to surface properties. Toxicology, 230, 90–104.

Weisenberger, D.J., Campan, M., Long, T.I., Kim, M., Woods, C., Fiala, E., Ehrlich, M. and Laird, P.W. (2005) Analysis of repetitive element DNA methylation by MethyLight. Nucleic Acids Res., 2;33(21):6823-36.

Yang, A.S., Estécio, M.R., Doshi, K., Kondo, Y., Tajara, E.H. and Issa, J.P. (2004) A simple method for estimating global DNA methylation using bisulfite PCR of repetitive DNA elements. Nucleic Acids Res., 18;32(3):e38.

You, J.S. and Jones, P.A. (2012) Cancer genetics and epigenetics: two sides of the same coin? Cancer Cell, 22: 9-20.

Figures

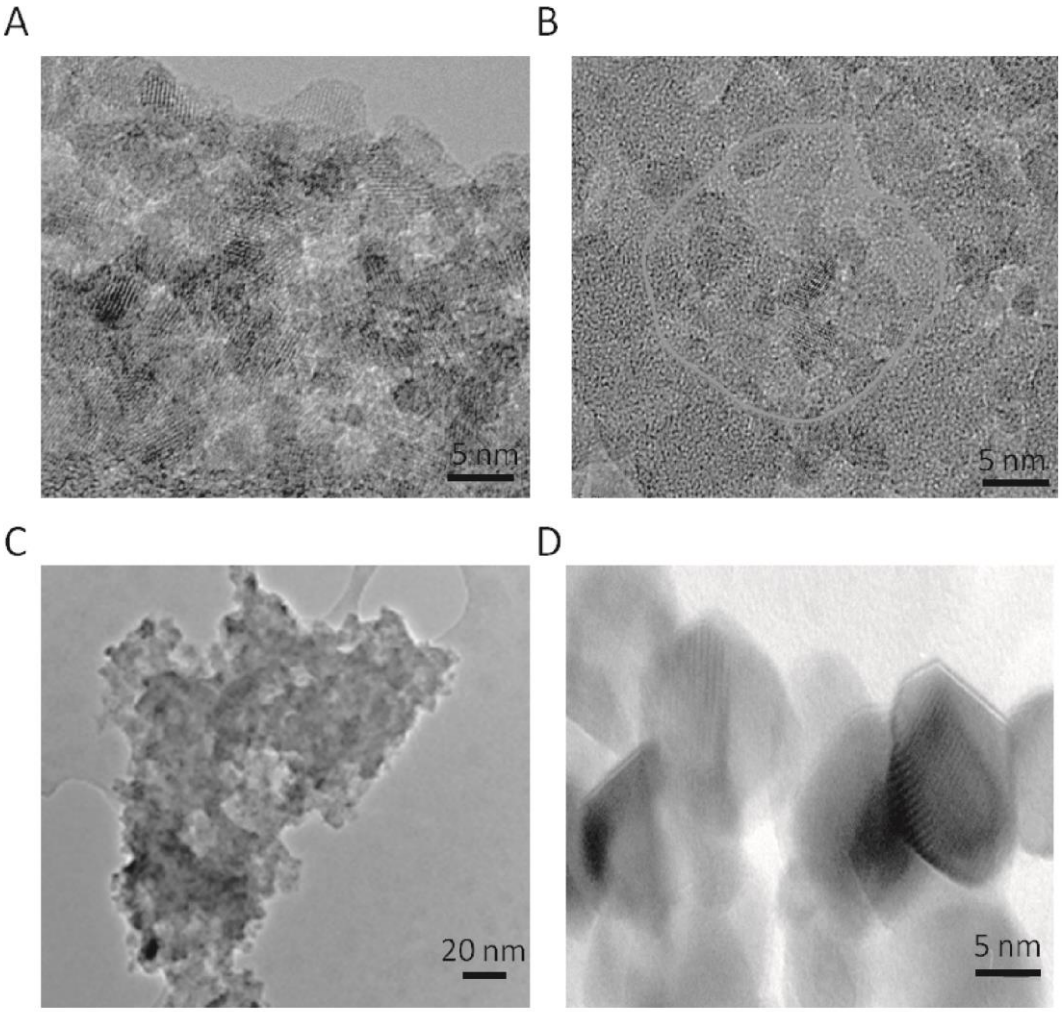

Figure 1. TEM images of TiO_2 NP. (A) pristine; (B) silica coated; (C) citrate coated; (D) P25.

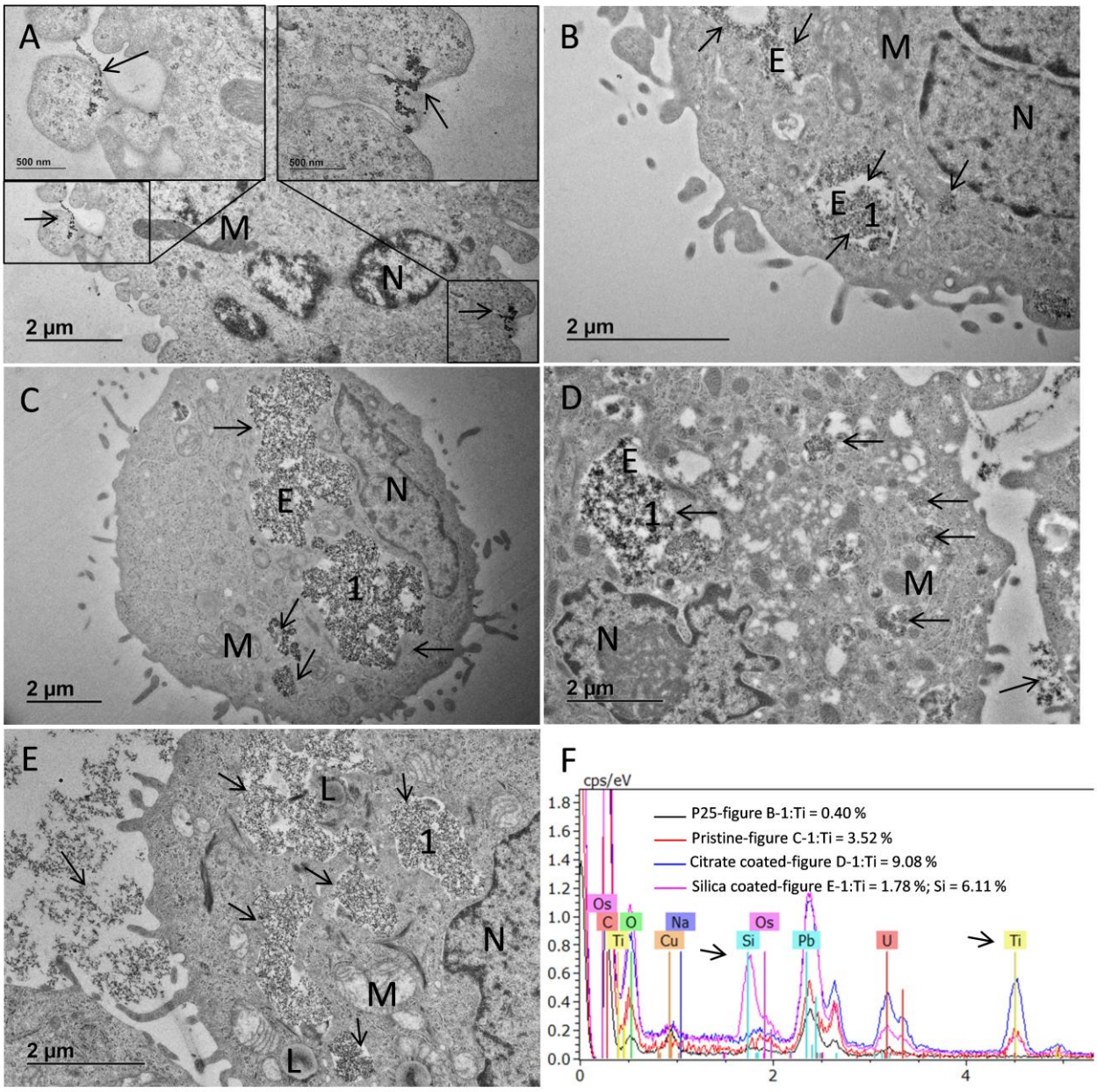

Figure 2. TiO_2 NP internalization: A549 cells analysed by TEM at 120 kV after 48 h of exposure to 20 µg/cm^2 of P25 (A: unspecific uptake mechanisms and NP in cytoplasm; B: NP inside endosomes);pristine (C); citrate coated (D); silica coated (E). Spectra obtained by EDS analysis confirmed the presence of Ti or Si, in case of silica coated NP, in areas n. 1 of each picture, measured at 120 kV in TEM mode. N: nucleus, M: mitochondria; E: endosome; L: lysosome; Arrows: NP.

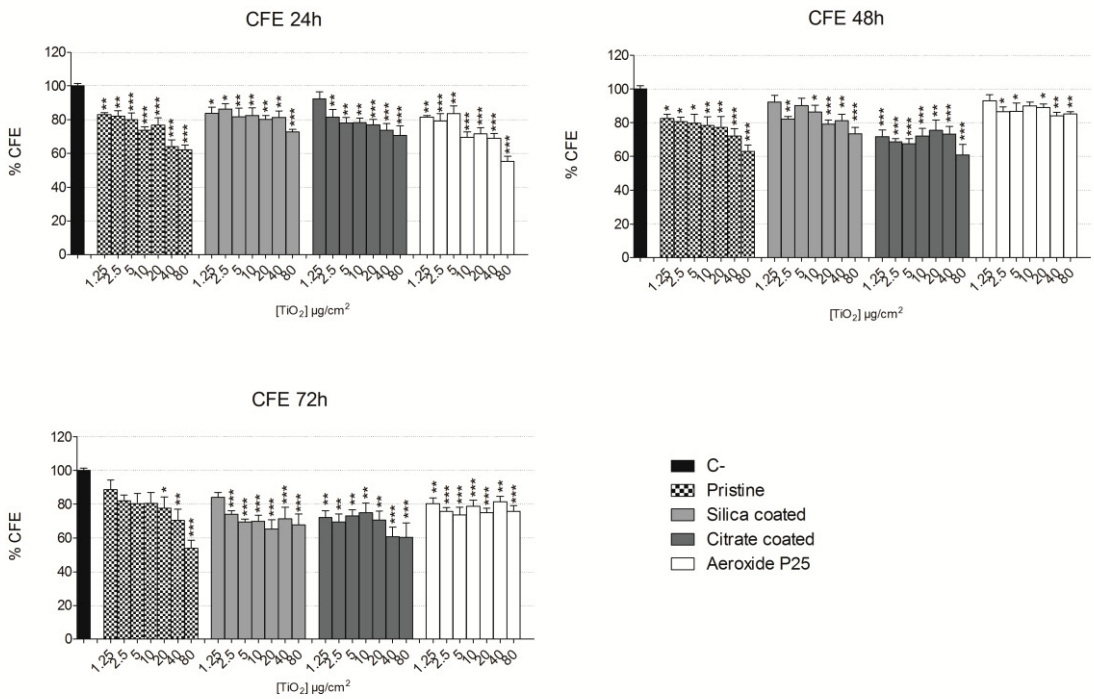

Figure 3. Cell viability in A549 cells exposed to TiO_2 NP evaluated by CFE assay. Cells were exposed to increasing concentrations (1.25–80 µg/cm^2) of NP for 24, 48 and 72 h. Data are plotted as mean %CFE values normalized to the untreated control (C-; black bar) ± standard error of the mean (SEM); n= 6. * P<0.05, ** P<0.01, *** P< 0.001. C+: 1000 µM Na_2CrO_4 that induced 0% CFE (data not shown).

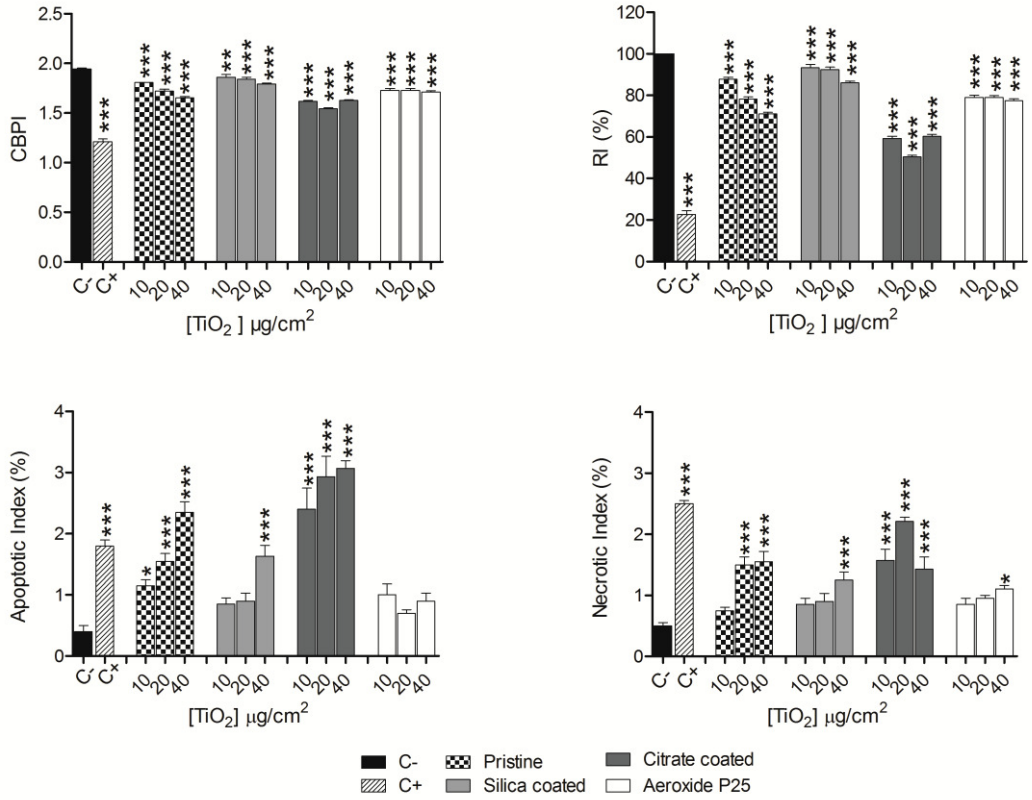

Figure 4. Cytostatic (CBPI and RI) and cytotoxic (apoptotic and necrotic index) effects induced by TiO_2 NP. Cells were exposed to increasing concentrations (10-20-40 µg/cm^2) of NP for 48 h. Data are plotted as mean values ± standard error of the mean (SEM); n= 4; statistical analysis performed by one-way ANOVA and Dunnet post-test.* $P< 0.05$, *** $P< 0.001$. As positive control 0.10 µg/ml mitomycin-C was employed.

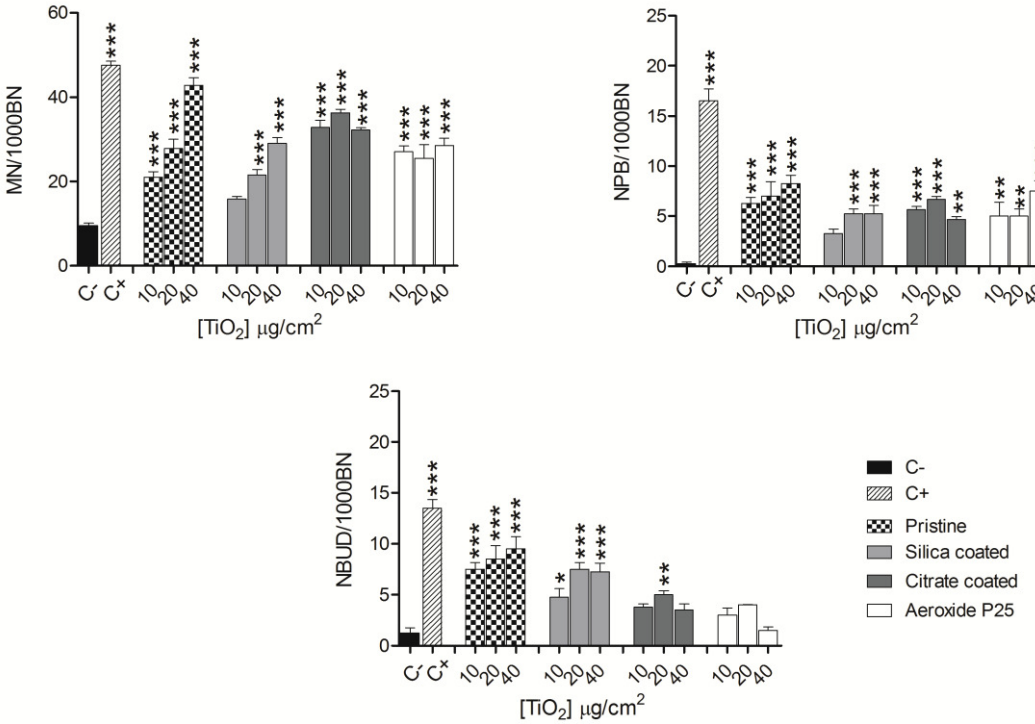

Figure 5. Chromosomal damage induced by TiO_2 NP. A549 cells were exposed to increasing concentrations (10-20-40 µg/cm^2) of NP for 48 h and MN, NPB and NBUD were manually scored using an inverted microscope (400X magnification). Data are plotted as mean values ± SEM; n = 4; statistical analysis performed by one-way ANOVA and Dunnet post-test. * $P<0.05$, ** $P<0.01$, *** $P<0.001$. As positive control 0.10 µg/ml mitomycin-C was employed.

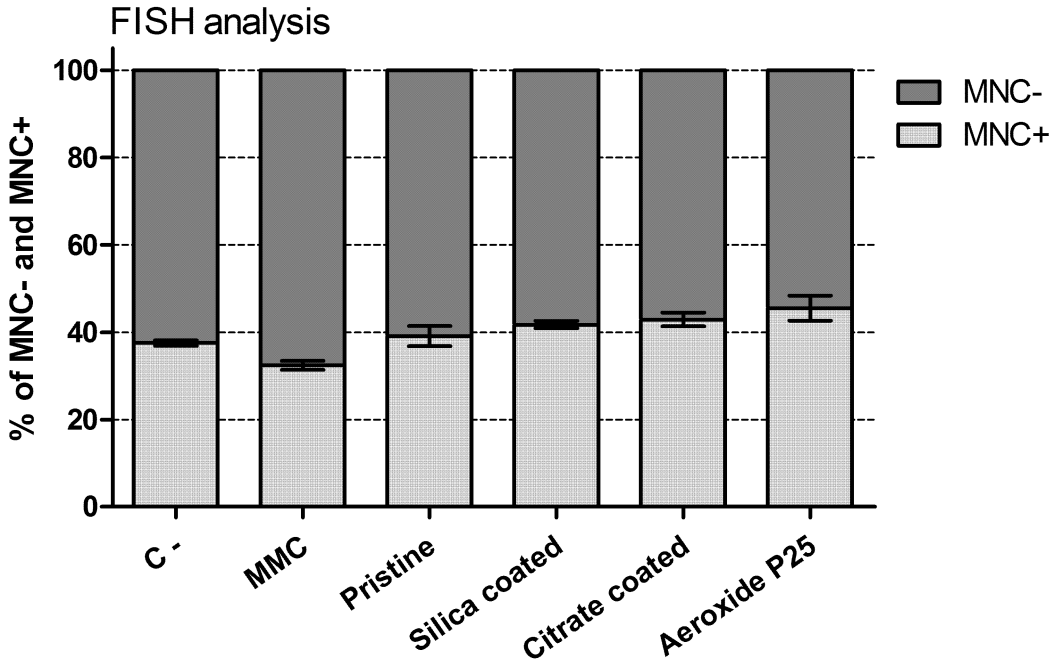

Figure 6. Fluorescence in situ hybridization (FISH) analysis with a pan-centromeric probe. Cells were exposed to 20 µg/cm^2 TiO_2 NP for 48 h. Mitomycin C (0.10 µg/ml) was used as clastogenic positive control. Data are presented as mean% ± SEM (mean of 4 replicates) of Cen+ (centromere positive) and Cen- (centromere negative). Statistical analysis was performed by *one-way* ANOVA and Dunnet post test.

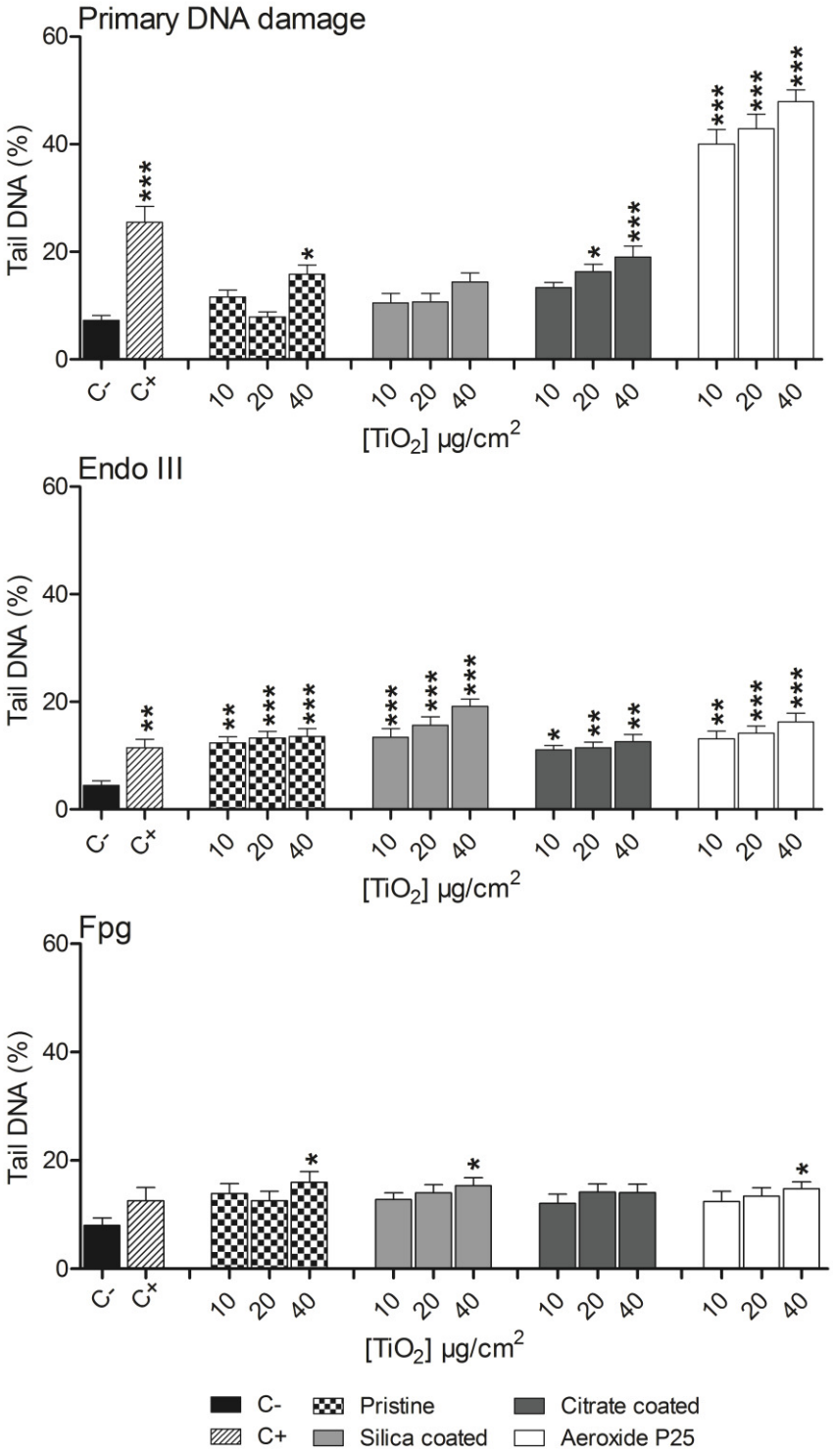

Figure 7. Primary and oxidised DNA lesions induced by TiO_2 NP in A549 cells treated for 48 h. The level of enzyme-sensitive sites was obtained by subtracting the value of % of DNA fluorescence in tail obtained after digestion with each enzyme and with the buffer only**.** Each data point represents the mean ±SEM of three independent experiments. C+: positive control (50 µM H_2O_2); C-: untreated control. Statistical analysis performed by one-way ANOVA and Dunnet post-test. * $P<0.05$; ** $P< 0.01$; *** $P<0.001$.

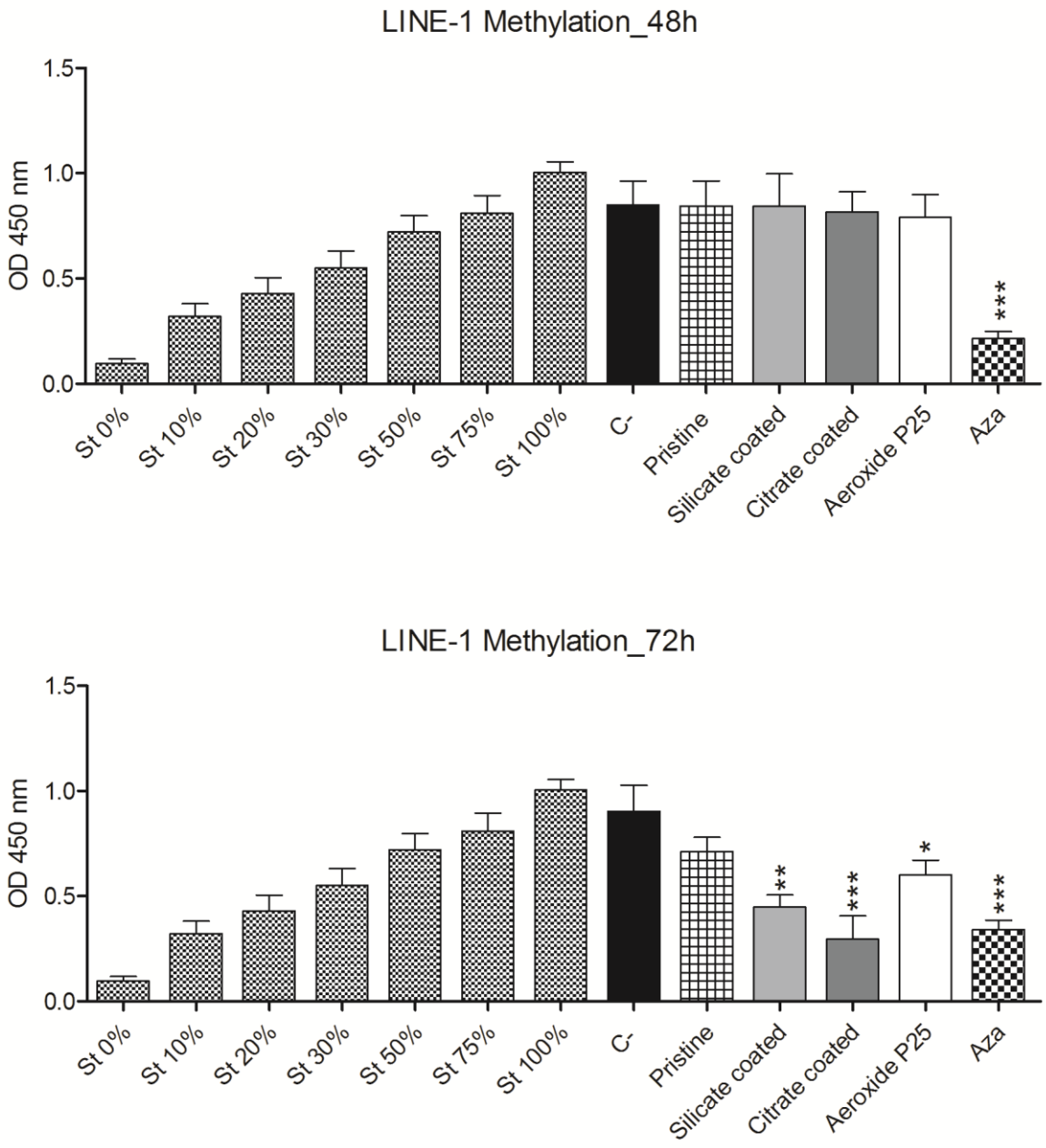

Figure 8. LINE-1 methylation levels of A549 cells after TiO_2 NP exposure. A549 cells were exposed to 40 µg/cm^2 of TiO_2 NP for 48 and 72 h. Each data point represents the mean ± SEM of three independent experiments. C-: untreated control; St: DNA standard with known methylation level. Aza: 5-Azacytidine. Statistical analysis performed by one-way ANOVA and Dunnet post-test. * P<0.05; ** P< 0.01; *** P<0.001.

Tables

Table 1.Mean hydrodynamic size by intensity and Zeta potential for 0.125 mg/ml of uncoated, citrated, silicated TiO_2 in deionized water.

TiO_2 NP	**Deionized water**				
	pH	**Z-pot (mV)**	**Mean size (nm)**	**PdI[#]**	**Fag***
Uncoated	2.33	41.2 ± 0.5	83.5 ± 10.4	0.48 ± 0.09	17
Citrated	5.47	-34.2 ± 1.2	57.5 ± 2.6	0.68 ± 0.05	11
Silicated	2.84	32.2 ± 4.1	155.6 ± 22.1	0.28 ± 0.01	-
Aeroxide® P25	4.13	37.4 ± 0.9	489.5 ± 130.5	0.30 ± 0.04	23

NP, and Aeroxide® P25 dispersed in deionized water. Data are reported as the mean ± standard deviation

PdI: polydisperisity index

* Fag (Agglomeration factor) was calculated by dividing DLS mean hydrodynamic diameter for TEM primary particles dimeter, that was calculated for uncoated sample around 5nm (Ortelli and Costa, 2016) and for P25 21nm as reported by Evonik provider. For sample dispersed in silica matrix it is difficult to calculate Fag because the system is formed by two different primary particles.

Table 2. Mean hydrodynamic size by intensity and Zeta potential for 0.125 mg/ml of uncoated, citrated, silicated TiO_2 in complete cell culture medium (Ham's F12).

TiO_2 NP	**Ham's F12**			
	pH	**Z-pot (mV)**	**Mean size (nm)**	**PdI[#]**
Uncoated	7.25	-10.6 ± 1.0	1608.0 ± 212.9	1.00 ± 0.0
Citrated	7.69	-10.3 ± 1.0	91.3 ± 6.3	0.27 ± 0.01
Silicated	7.56	-10.6 ± 0.4	563.2 ± 84.0	0.80 ± 0.1
Aeroxide® P25	7.74	-10.2 ± 0.2	477.0 ± 8.1	0.47 ± 0.02

NP, and Aeroxide® P25 dispersed in complete cell culture medium (Ham's F12). Data are reported as the mean ± standard deviation.

PdI: polydisperisity index

Table 3. TiO_2 NP effects on different endpoints.

Endpoint	**Nanoparticles**			
	Pristine TiO_2	Silicated TiO_2	CitratedTiO_2	Aeroxide P25
Cellular uptake	Yes	Yes	Yes	Yes
CFE	**++**	**++**	**+++**	**+**
CBPI/RI	**+++**	**+++**	**+++**	**+++**
Apoptotic	**++**	**+**	**+++**	**-**
Necrotic	**++**	**+**	**+++**	**+/-**
MN	**+++**	**++**	**+++**	**+++**
NPB	**+++**	**++**	**+++**	**++**
NBUD	**+++**	**++**	**+/-**	**-**
FISH	Cen-	Cen-	Cen-	Cen-
PrimaryDNA damage (Comet)	**+/-**	**-**	**++**	**+++**
Oxidative DNA damage (Endo III)	**+++**	**+++**	**++**	**+++**
Oxidative DNA damage (Fpg)	**+/-**	**+/-**	**-**	**+/-**
LINE-1 hypomethylation	**-**	**+**	**++**	**+/-**

The symbol "-" indicate that no significant effect was found. "+" represents a low increase, and "+++" a high increase. The symbol "+/-" indicates that the positive effect was found only in a single experimental point. Cen- = formation of centromere negative micronuclei.